Table 1. OPO performance at room-temperature.

poling period (μm)	threshold pump power (mW)	OPO wavelength signal (μm)	idler (μm)	output power signal (mW)	idler (mW)	pulsewidth signal (fs)	idler (fs)
29.5	280	2.25	4.84	20	20	295	400
30.5	160	2.35	4.56	24	22	163	510
31.5	165	2.43	4.33	60	59	133	492
32.5	155	2.48	4.08	37	50	110	470

The PPLN crystal is mounted inside an oven to allow for a fine tuning of the OPO emission frequency; for brevity temperature tuning curves are not reported in this paper, and experimental data refer to room temperature. The combination of different poling periods with temperature tuning allows for a stepwise coverage of the OPO peak wavelengths (continuous tuning needs a crystal with fan out grating [6]). The signal and idler spectra, acquired using a scanning monochromator with a resolution bandwidth (RBW) of 0.5 nm and a PbSe photodiode, are reported in Fig. 2(a) for the poling periods available from 29.5 to 32.5 μm. The corresponding signal and idler wavelengths cover the range 2.25-2.6 μm and 4.1-4.9 μm, respectively, with a maximum spectral width of 100 nm at 2.48 μm. Due to strong water vapor resonances in the 2.55-2.7 μm range, it was not possible to drive the OPO above threshold with the remaining poling periods. Figure 2(b) shows the average power and pulse duration of the signal and idler as a function of the central wavelength for each spectrum. The power levels are in the range 20-60 mW, with a maximum of 60 mW for both signal and idler when using the 31.5 μm poling period. The pulse durations have been measured by an interferometric autocorrelator based on collinear second harmonic generation in a $LiIO_3$ crystal. Figure 2(c) shows the autocorrelation trace of the signal pulse train with the minimum duration of 110 fs (40-mW power), as retrieved by a fit assuming a $sech^2$-pulse shape, corresponding to a time-bandwidth product of 0.46. The reduction of the signal bandwidth when changing the poling period is due to the decrease of the phase-matching acceptance bandwidth and to the reduced transmission of the PPLN crystal (cut-off at $\sim$5 μm), which introduces increasing losses on the idler. This is also confirmed by the trend of the power levels, with the exception of the data corresponding to the 32.5-μm poling, where the reported values are affected by the water vapour absorption at 2.55 μm. Table 1 summarizes the OPO performance.

3. OPO intensity stabilization

The long-term stabilization of the signal intensity has been achieved by exploiting the wide spectrum of nonlinear mixing signals generated by non phase-matched interactions inside the PPLN crystal with a technique similar to that described in [6]. Figures 3(a) and 3(b) show the nonlinear tones extracted from the HR plane mirror of the OPO cavity in the visible and near infrared spectral regions, respectively. Each tone has been labelled according to the specific nonlinear process involved (e.g. $p+i$ represents the sum frequency between the pump and idler comb). The beam is dispersed using a fused silica prism and focused onto a 125-MHz InGaAs photodiode after proper spectral filtering by a slit. The spectral overlap around 1200 nm between the components $p+i$ and $2s$ gives rise to a beatnote at $f_0^p + f_0^i - 2f_0^s = 2f_0^p - 3f_0^s$, where f_0^p, f_0^s and f_0^i are the offset frequency of the pump, signal and idler, respectively. The same beat frequency has been observed around 600 and 800 nm, originating from the overlap of $2p+s$ with $4s$, and $2p$ with $3s$, respectively. A phase-lock circuit was implemented to stabilize the beatnote against a 15-MHz reference derived from a frequency synthesizer. The signal at the

#171989 - $15.00 USD Received 10 Jul 2012; revised 30 Aug 2012; accepted 6 Sep 2012; published 11 Sep 2012

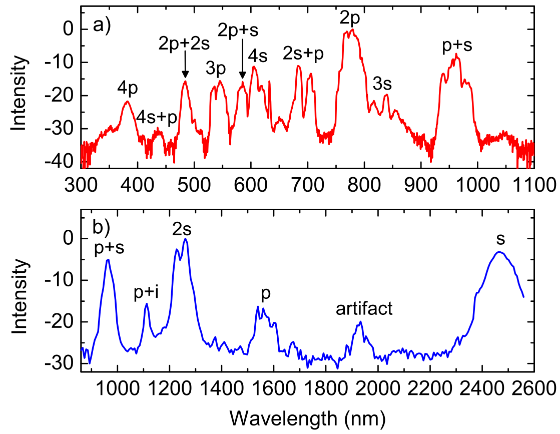

Fig. 3. Nonlinear tones simultaneously generated by the OPO in the visible (a) and near-infrared (b) spectral region. The labels have been assigned according to the nonlinear phenomena corresponding to each tone.

output of the InGaAs photodiode has been suitably amplified (∼30 dB) to match the input dynamic of the phase detector, and then sent to a proportional-integral servo acting on a piezo mounted cavity mirror. The signal radiation is constituted by frequencies $\nu_k^s = kv/L = kf_r + f_0^s$, where k is the number of wavelengths within the cavity, v is the mean phase velocity, L is the cavity length, and f_r is the repetition frequency. Since the OPO signal is inherently synchronous with the pump, a change in the cavity length at constant f_r induces only a change of f_0^s [15]. Therefore, phase-locking of this beat note translates into an OPO cavity length control, providing long-term stabilization of the OPO signal intensity.

Figure 4 shows the locked beatnote as measured with an RF spectrum analyzer. The observed FWHM of 38 kHz is consistent with the free-running width of the pump offset frequency f_0^p, which is not controlled in this experiment. The beatnote in Fig. 4 has been acquired using the 32.5 μm poling period. Similar results in terms of FWHM with slightly reduced peak values

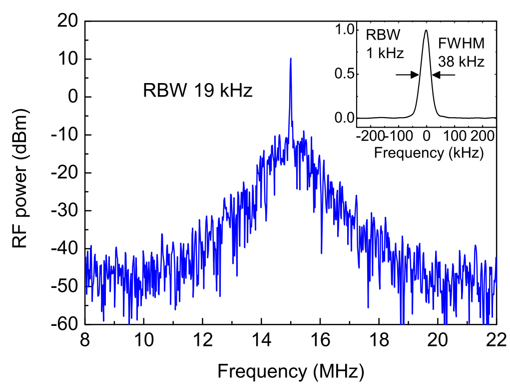

Fig. 4. RF spectrum of the beatnote between the 3s and 2p tones extracted from the OPO cavity, locked to a 15-MHz reference. Inset: detail of the locked beatnote.

#171989 - $15.00 USD Received 10 Jul 2012; revised 30 Aug 2012; accepted 6 Sep 2012; published 11 Sep 2012

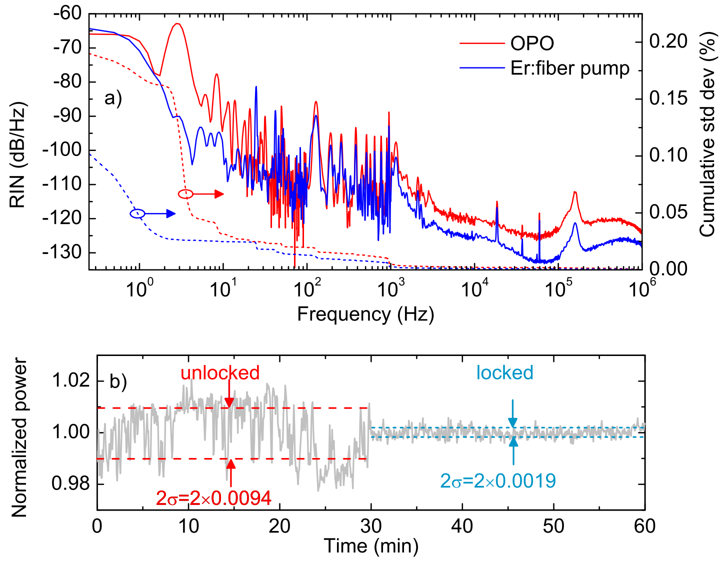

Fig. 5. (a) RIN (left) and cumulative standard deviation (right) of the locked OPO and Er-fiber pump laser. (b) Signal intensity versus observation time for unlocked (0–30 min) and locked OPO (30–60 min).

have been obtained for all remaining periods, due to the good spectral overlap between the $p+i$ and $2s$ nonlinear tones. Figure 5(a) shows the relative intensity noise (RIN) of the signal, as recorded by an extended-InGaAs photodiode with 10-MHz bandwidth, when the OPO cavity length is locked. For comparison, the RIN of the Er-fiber pump oscillator is also shown. For Fourier frequencies lower than 20 Hz and larger than 1 kHz an excess noise in the OPO RIN is observed, due to conversion of the pump offset frequency phase-noise into OPO amplitude noise [10, 16] and cavity vibrations. The cumulative standard deviation of the OPO intensity is as low as 0.2%, *i.e.* a factor of $\sim$2 larger than the pump laser cumulative standard deviation of 0.1%. Long-term intensity stability of the OPO signal is also shown in Fig. 5(b) for 1 h observation time. The free running standard deviation of the OPO intensity is effectively reduced by a factor $\sim$5 when the active stabilization loop of the OPO cavity length is closed.

4. Conclusion

In conclusion, a compact OPO source synchronously pumped by a commercial 250-MHz Er:fiber laser has been presented. The OPO signal and idler cover the spectral range 2.25-2.6 μm and 4.1-4.9 μm, respectively, with average powers from 20 to 60 mW. The minimum observed pulse duration is 110 fs at 2.5 μm, with a power level of 40 mW. In addition, long-term active stabilization of the signal intensity in the whole tunability range from 2.25 to 2.6 μm allows for the reduction of the intensity noise down to the 0.2% level. Further stabilization of the pump repetition and offset frequencies will lead to a full mid-IR comb source, which could be used for absolute referencing of solid-state Cr^{2+} lasers and quantum cascade lasers, or for direct comb spectroscopy in the mid-IR spectral region.

Acknowledgment

The authors acknowledge financial support from the Italian Ministry of University and Research, ELI infrastructure.